Chinese Chemical Letters 32 (2021) 1765–1769

Contents lists available at ScienceDirect

Chinese Chemical Letters

journal homepage: www.elsevier.com/locate/cclet

Communication

Glutathione-triggered non-template synthesized porous carbon nanospheres serve as low toxicity targeted delivery system for cancer multi-therapy

Haoyuan Lv[a], Shuai Ma[a], Zhenbo Wang[a], Xiaoting Ji[a], Shaoping Lv[b], Caifeng Ding[a,b,*]

[a] Key Laboratory of Optic-Electric Sensing and Analytical Chemistry for Life Science, Ministry of Education, Shandong Key Laboratory of Biochemical Analysis, Key Laboratory of Analytical Chemistry for Life Science in Universities of Shandong, College of Chemistry and Molecular Engineering, Qingdao University of Science and Technology, Qingdao 266042, China
[b] Qingdao Central Hospital, Qingdao 266042, China

ARTICLE INFO

Article history:
Received 3 October 2020
Received in revised form 23 November 2020
Accepted 24 November 2020
Available online 3 December 2020

Keywords:
Cell imaging analysis
Drug delivery
Biothiol sensing
Low biotoxicity
Porous carbon

ABSTRACT

Nanomaterial based drug delivery system have received great attention in clinical application due to their high therapeutic efficacy and lower side effects than classical method, multi-functional nanomaterial also have shown the excellent performance at cancer theranostic and durg tracking *in vivo* and *in vitro*. However, most of these works are influenced by the bio-toxicity of applied nanomaterials, which could influence the diagnostic results and treatment effect. Therefore, we have prepared a high biocompatibility porous carbon nanospheres (PCNs) based nano-system (PCN-siRNA-DOX-FA) for targeted drug delivery and theranostic. The surface modifications have increased dispersion and stability of the PCNs, and folic acid (FA) had enhanced the active target ability for FA receptor positive cell lines. Moreover, through the siRNA structure and doxorubicin (DOX) loading, biological and chemical combined multi-therapy was achieved in cancerous cells. This constructed nano-system could positively improve the biotoxicity problem of nanomaterial and provide a potential platform for clinical cancer theranostic applications.

Similar to epidemic viral diseases, cancer is still a major problem that expected to be solved for human [1,2]. At present, the majority of cancer treatments are general based on surgery and chemotherapy [3,4]. Although these classic methods are effective and easy to be achieved in clinical application, some problems such as the identification of tumor tissue boundaries in surgery or the real-time response to the drug behavior in treatment are still needed improvement. Moreover, cancer resistance and distant metastasis also become more and more serious in clinical treatment [5–7]. All of these suggested that we have needed a new method for surgery guidance, and more effective way for drug delivery and treatment. On the basis of previous research, the nanomedicine was primary proposed by nanotechnology-based drug delivery systems (DDSs) [8,9]. Under this theory, a large number of DDSs were constructed by functional nanomaterials such as nano-gold particles, multi-metal doped quantum dots and metal organic frame (MOF) have been reported with excellent performance [10–14]. However, as the cornerstone of DDSs, enhanced permeability and retention effect (EPR effect) based passive transport is the crucial rule for the *in vivo* transport of these nanomaterials, which leads to the risk of non-specific accumulation *in vivo* [15], therefore, the bio-toxicity performance of applied nanomaterials is quite considerable.

As emerging materials, porous carbon nanospheres (PCNs) had a wide range of applications such as energy storage or catalysis application [16,17]. In particular, their toxicity and surface modification performance could have potential in biological and biomedical applications [18]. However, the classical preparation routes of PCNs were usually based on template-method, the tedious operation and low yields have limited their practical uses [19]. Therefore, the non-template synthesized method was faster and cheaper than classical method, which was more suitable for practical preparation applications. Wan *et al.* have reported a structure controllable synthesized routes for PCNs by

* Corresponding author at: Key Laboratory of Optic-Electric Sensing and Analytical Chemistry for Life Science, Ministry of Education, Shandong Key Laboratory of Biochemical Analysis, Key Laboratory of Analytical Chemistry for Life Science in Universities of Shandong, College of Chemistry and Molecular Engineering, Qingdao University of Science and Technology, Qingdao 266042, China.
E-mail address: dingcaifeng2003@163.com (C. Ding).

https://doi.org/10.1016/j.cclet.2020.11.058
1001-8417/

non-template method, and applied for potassium-ion battery [20]. Our previous work has also been realized the detection and analysis of adenosine triphosphate (ATP) in living cells based on non-template synthesized PCNs [21]. In this work, we hope to apply it further in integrated diagnosis and treatment application with the advantages of its low toxicity performance.

Compared with traditional medicines, another advantage of nanomedicine have shown in the diversification of treatment modalities, not only can use the loaded drugs for chemical treatment, but also make full use of its physical and chemical properties for other treatment such as photothermal treatment, photoacoustic treatment and radio sensitization treatment, which had been widely reported in recent years [22–25]. It is obvious shown that the multimodal treatment strategy has a significant advantage than single drugs. However, the multimodal treatment strategy has also increased the patient's risk of drugs side effects, so it requires better safety and active targeting ability in carrier materials to reduce side effects on normal tissues *in vivo*. Most of them are achieved through the design of the cell microenvironment response structure and tumor target recognition components [26–28]. For instance, Zhu *et al.* have reported a peptide-modified hollow mesoporous system to realize the microenvironment response based multi-therapy [29]. Lu *et al.* have used the ligand-modified cell membrane to achieve the targeted drug nanocrystals delivery [30]. Moreover, low-toxic materials constructed drug delivery systems with multiple recognition responses of cell membrane receptors and intracellular environment will have more outstanding clinic application capabilities.

Herein, we have constructed a glutathione-triggered drug delivery system by non-template method synthesized PCNs, which achieved the response tracing for bio-thiols and targeted multi-therapy for cancer cells. The PCNs and surface modification processes were shown in Scheme S1 (Supporting information). The activated SPDP modified N-PCNs were coupling with sulfydryl-labelled siRNA structure and loaded with chemotherapy drugs doxorubicin (DOX), which was designed for multi-therapy by siRNA based biotherapy and DOX based chemotherapy, the selected siRNA sequence could induce cancer cell apoptosis by Axl signal pathway silencing [31], folic acid (FA) was conjugated on N-PCNs surface to achieve the FA receptor mediated targeted delivery for FA receptor high expressed cancerous cells. As shown in Scheme 1, when encountering target cells, the conjugated FA could specifically bind to the FA receptors that expressed on target cell membrane and induced cell internalization process. Due to the high expression of the bio-thols in the cancerous cells, the loaded DOX was released to realize the chemotherapy and siRNA was released to form RNA-induced silencing complex for biotherapy with the cleavage response of disulfide bonds, which completed multi-therapy for targeted cancer cells *in vivo* and could also achieve the bio-thols detection *in vitro*. Meanwhile, the FA recognition process and bio-thiols response process formed a double protection mechanism, to ensure the loaded cargos were released in target cells with high expressed FA receptors and special intracellular environment, which further reduced the toxic damage on normal tissues or organs by off-target effects.

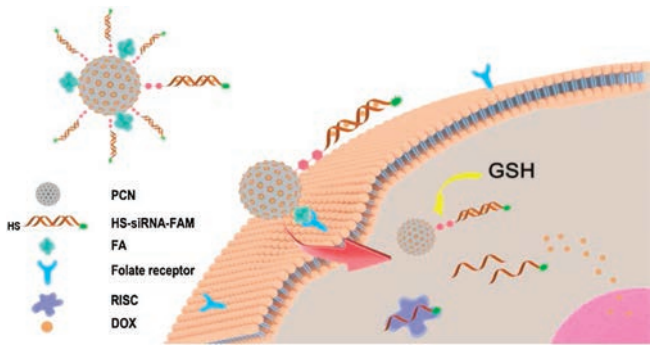

Scheme 1. Schematic illustration showed the multi-therapy process by bio-thiols response mediated drug release in FA receptor high expressed cells.

The images of transmission electron microscopy (TEM) have clearly showed the formation and structures of PCNs, with a number-average diameter of 284.5 ± 3.1 nm (Fig. 1A, image a). After surface oxidation and amino modified treatment, the morphology of PCNs have not changed significantly, the N-PCNs (Fig. 1A, image c) was little larger than O-PCNs (Fig. 1A, image a) with an average diameter of 295.5 ± 4.1 nm than 287.5 ± 2.8 nm, resulting from the surface silicon deposition process during the amino modification. The Raman spectra of PCNs, O-PCNs and N-PCNs have also shown two characteristic peaks of the carbon nanomaterial, G-band (1576 cm^{-1}) and D-band (1350 cm^{-1}) (Fig. S1 in Supporting information). The surface modification not only provided a basis for subsequent assembly, but also improved the PCNs dispersion and stability in solution. The N-PCNs gained the better performance (Fig. S2 in Supporting information).

As shown in (Fig. 1A, image d), the average diameter of assembled N-PCNs complex (PCN-siRNA-DOX-FA) was 445 ± 5.2 nm and observed a hydrogel like shell around the PCNs core, which suggested that the nucleic acid and folic acid (FA) based bio-recognition part was constructed on the N-PCN surface expectantly. Furthermore, the energy dispersive spectroscopy (EDS) mapping image analysis was used to investigate the component of the PCN-siRNA-DOX-FA complex (Fig. 1B), and it shown that the nanospheres mainly contains C, O, N, Si and P elements. Among them, the O, N and P elements distribution on shell surface were observed, caused by the siRNA structure and (3-aminopropyl)-triethoxysilane (APTS) amination expectantly modified on PCNs, to indicate the surface modification were successfully attached to the PCNs. UV–vis absorption spectrum was applied to characterize the DOX loading condition (Fig. 1C), similar to the pure DOX (Fig. 1C, curve b), PCN-siRNA-DOX-FA (Fig. 1C, curve c) have shown a significant absorption intensity of DOX at 495 nm compared with that of PCN-siRNA-FA (Fig. 1C, curve a), which suggested that DOX was effective loaded, and the loading amount of DOX was calculated about 122 μg/mg (Fig. S3 in Supporting information).

In addition, the change of zeta potential also proved the surface modification process (Fig. S4 in Supporting information), based on the protonation of amino groups, N-PCNs have shown more negative charge in the buffer solution than that of O-PCNs. As shown in (Fig. 1D), the surface modification of siRNA structure have made N-PCNs negatively charged (Fig. 1D, image a), the positively charged DOX could make siRNA structure more tight by the charge interaction, and the FA made the tight structure not too dense, which was beneficial for the cell uptake and molecular recognition. The dynamic light scattering (DLS) was applied to characterize the nanoparticle form in solution (Fig. 1E), the hydrodynamic diameter of PCN-siRNA-DOX-FA (463.5 ± 7.6 nm) was between PCN-siRNA-DOX (375.5 ± 6.3 nm) and PCN-siRNA (496.5 ± 7.2 nm), larger than N-PCNs (315.5 ± 4.3 nm), due to the dehydration of the functional surface modification in vacuum environment and alteration in liquid solution, particle diameters were much larger than those obtained in TEM measurements.

To investigate the biological toxicity, double staining flow cytometry method was applied. Hela cells were co-cultured with different concentrations of N-PCNs for 5 h. As shown in Fig. 2A, even at a slightly high concentration, it still maintained a better cell survival rate (around 80%), which proved an acceptable bio-compatibility and cytotoxicity for cellular application. In addition, the long term measurement by DLS was applied to confirm the PCN-siRNA-DOX-FA complex stability in solution, the different pH

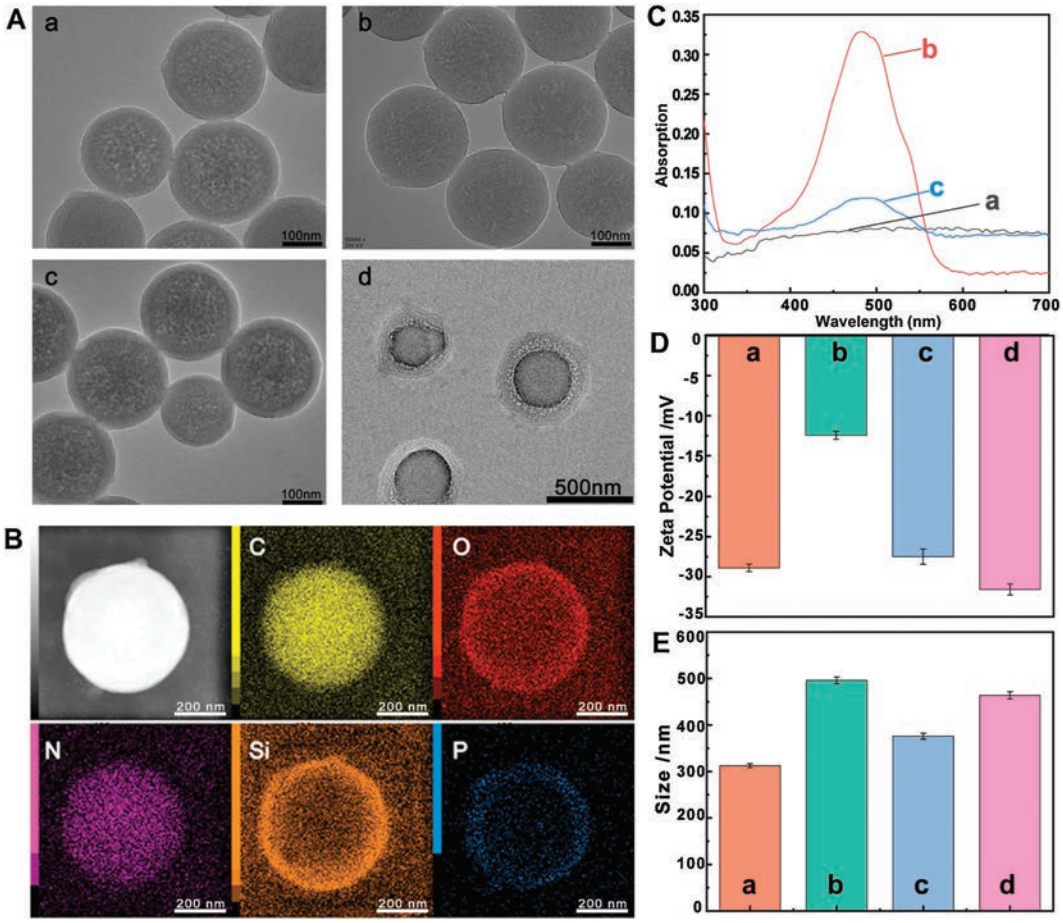

Fig. 1. (A) TEM images of PCNs (a), O-PCNs (b), N-PCNs (c) and PCN-siRNA-DOX-FA complex (d). (B) TEM image and EDS mapping information of the constructed PCN-siRNA-DOX-FA complex. (C) UV–vis absorption spectra analysis of PCN-siRNA-FA (a), pure DOX (b) and PCN-siRNA-DOX-FA complex (c). (D) The zeta potential analysis of PCN-siRNA (a), PCN-DOX-FA (b), PCN-siRNA-DOX (c) and PCN-siRNA-DOX-FA (d) in PBS buffer solution (10 mmol/L, pH 7.4). (E) The DLS analysis of N-PCNs (a), PCN-siRNA (b), PCN-siRNA-DOX (c) and PCN-siRNA-DOX-FA (d) in PBS buffer solution (10 mmol/L, pH 7.4). Error bars indicate SD ($n = 5$).

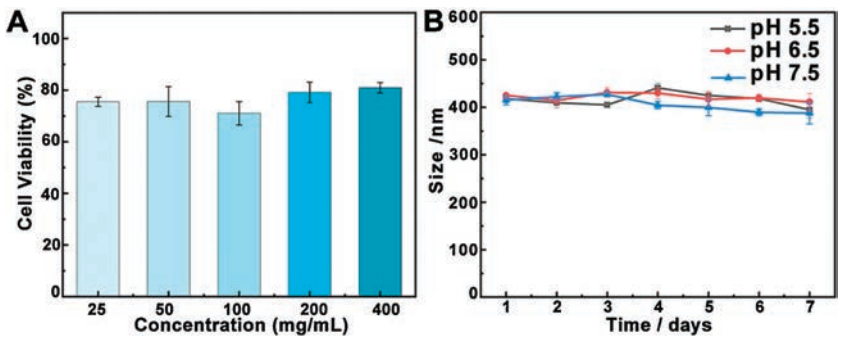

Fig. 2. (A) Cell viability of Hela cells co-cultured with different concentrations of N-PCNs for 5 h, detected and analysis by flow cytometry. (B) The long term DLS stability analysis of PCN-siRNA-DOX-FA complex in different pH PBS buffer solution form 1 day to 7 days. Error bars indicate SD ($n = 5$).

buffers were choose to simulate the body and cell micro-environment. In Fig. 2B, during the 7 days test, slightly changes were observed in the size of the particles, which proved a better stability in solution, especially at the environment of pH 7.4 shown more stable than the weakly acidic cancer cell environment, that is beneficial for *in vivo* delivery process. To confirm the response ability of the PCN-siRNA-DOX-FA complex toward bio-thiols, such as glutathione (GSH) *in vitro*, kinetic studies were carried out with different concentrations of GSH. The relative fluorescence intensity was found in a linear relation with the concentration of GSH in the range of 100 μmol/L to 2.5 mmol/L, and the limit of detection (LOD) was calculated to be 65 μmol/L, which could meet the needs of early detection and analysis of bio-thiols in cells (Fig. S5 in Supporting information).

The confocal laser scanning microscopy (CLSM) was applied to investigate the cellular uptake and bio-interaction of surface

modification on PCN-siRNA-DOX-FA complex, the fluorescence of FAM and DOX was used to study the cellular uptake and interaction status. DOX and FAM presented different imaging morphology through their different biological effect. DOX was more concentrated in the nucleus structure in cells, while FAM was present in the cytoplasm with the modified siRNA. Hela cells were co-cultured with PCN-DOX-FA, PCN-siRNA-FA, PCN-DOX-siRNA and PCN-siRNA-DOX-FA for 5 h. As shown in Fig. 3, although the DOX channel of PCN-DOX-FA group have shown red fluorescent signal under the FA mediated cellular uptake, the weaker fluorescent signal indicated that the low loaded amount of DOX due to the lack of siRNA structure modification. Meanwhile, the stronger green fluorescent signal of FAM channel was observed in PCN-siRNA-FA group, which proved the complex was uptake and released in the cytoplasm. However, without FA modification, PCN-DOX-siRNA group have shown the nearly black fluorescent signal both in FAM and DOX channel, which suggested the cellular uptake rate correlation with FA. On the other hand, relative to PCN-DOX-FA and PCN-siRNA-FA, PCN-siRNA-DOX-FA group have shown more stronger fluorescence intensity in both FAM and DOX channel, indicated that the delivery efficacy was mostly depended on the assistance of FA, and the release process of bio-thiols response could further reduce the effect of aggregation-induced quenching (ACQ) effect on fluorescence intensity. Furthermore, PCN-siRNA-DOX-FA complex co-cultured with the folic acid receptors low-expressed cell lines (MCF-7, HUVEC), also shown the lower fluorescent signal in FAM and DOX channel (Fig. S6 in Supporting information), proved the internalization of complex into targeted cells was occurred when surface was modified with FA and FA receptors were available on target cells.

To confirm the therapeutic effect of constructed complex *in vitro*, Hela cells were co-cultured with N-PCNs, PCN-siRNA, PCN-siRNA-FA, PCN-DOX-FA, PCN-siRNA-DOX, PCN-siRNA-DOX-FA from 1 h to 5 h respectively, double staining flow cytometry was applied to characterize the cells status after co-cultured. N-PCNs have shown lower cytotoxicity during the culture process (Fig. S7A-a in Supporting information). The surface modification of siRNA structure had an obvious therapeutic effect (Fig. S7A-b in Supporting information) than unmodified group (Fig. S7A-c in Supporting information), indicated the released siRNA could continue produce cellular effects on tumor treatment. Conjugated with FA was still an important factor affecting delivery efficiency (Fig. S7A-b, Fig. S7A-c, Fig. S7A-e and Fig. S7A-f in Supporting information), meanwhile, without the blocking effect of siRNA structure, even with the targeted modification of FA, PCN-DOX-FA still obtained a worse therapeutic effect compared to other groups, suggested the load of DOX is related to the surface blocking structure (Fig. S7A-d in Supporting information). PCN-siRNA-DOX-FA complex showed a better performance even at 3 h, which proved the combined treatment strategy more effective than single drug therapy. In addition, in order to further investigate the cellular effect process of PCN-siRNA-DOX-FA complex, CLSM system was used as a continuous observation analysis from 1 h to 5 h. With the time increasing, the fluorescent signals of FAM and DOX channel were gradually enhanced, and could be observed significantly at 3 h, that indicated the PCN-siRNA-DOX-FA complex could be damaged by thiols in the living cells and released the cargo progressively (Fig. S8 in Supporting information). On the other hand, the morphology changes of cells were also observed in bright and merge channels.

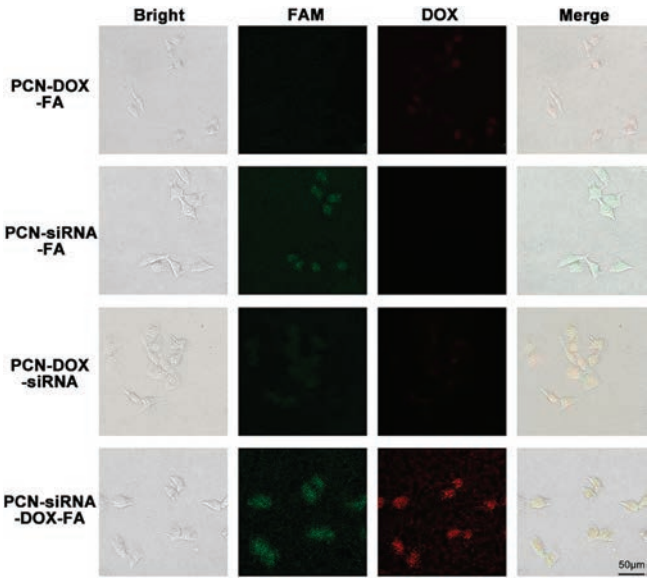

Fig. 3. (A) Confocal laser scanning microscopy (CLSM) images of Hela cells, after co-cultured with PCN-DOX-FA, PCN-siRNA-FA, PCN-DOX-siRNA and PCN-siRNA-DOX-FA for 3 h in bright channel, fluorescence channel and merged images. Scale bars of images are 50 μm.

To evaluate the therapeutic effect of PCN-siRNA-DOX-FA complex *in vivo*, Hela tumor-bearing mice were intravenously injected with PCN-siRNA-DOX-FA and PBS (as untreated negative control). The fluorescence signal could be maintained after injection of PCN-siRNA-DOX-FA, proving the complex serves as an effective platform for drug release and analysis (Fig. 4A). In order to confirm the distribution and biological toxicity in internal organs, the heart, lung, liver, spleen and kidney of the mice were dissected out for observation. Compared with PBS treatment group, main organs in PCN-siRNA-DOX-FA treatment group (Fig. 4B) have shown low fluorescent signals, except for tumor tissue. Due to the metabolic effect of the organism, there was a weak fluorescence signal in the liver and kidneys, which proved the targeted delivery and controlled release of PCN-siRNA-DOX-FA complex was effective and could effectively reduce the toxicity to normal organs. Moreover, the tumor volume and body weight of the mice were measured during the experiment, the growth trend of PCN-siRNA-DOX-FA group (Fig. 4C, curve b) had slowed down significantly than PBS control group (Fig. 4C, curve a), and there was a slow trend turning point observed on the 7th day, which proved the constructed complex played an effective therapeutic on inhibition the growth of tumor *in vivo*, and after a long period of treatment (7 days). Moreover, during the experiment, treatment group (Fig. 4D, curve b) and the control group (Fig. 4D, curve a) showed similar growth trends, and the body of the treatment group was slightly lighter than the control group, suggested that the PCN-siRNA-DOX-FA complex had no effect on the normal growth of mice, while inhibiting tumor growth. Overall, these results indicate the significance of constructed glutathione-triggered PCN-siRNA-DOX-FA complex for *in vivo* applications.

In summary, we have constructed a double protection multi-therapy strategy by low toxicity porous carbon nanospheres, achieved bio-thiols sensing *in vitro* and drug controlled release *in vivo*. Compared with traditional methods, PCNs exhibited better biocompatibility and non-template method was easier for large amount preparation in reality. Meanwhile, the thiol-responsive siRNA structure realized the effective blocking and release control of the loaded cargo that would be helpful for improving the stability of the circulation in the body. Functionalized with FA was also obtained a nice performance on target recognition, that could ensure the loaded cargos were released in target cells with high expressed FA receptors and special intracellular environment, which further reduced the toxic damage on normal tissues or organs by off-target effects. Moreover, the PCN-siRNA-DOX-FA

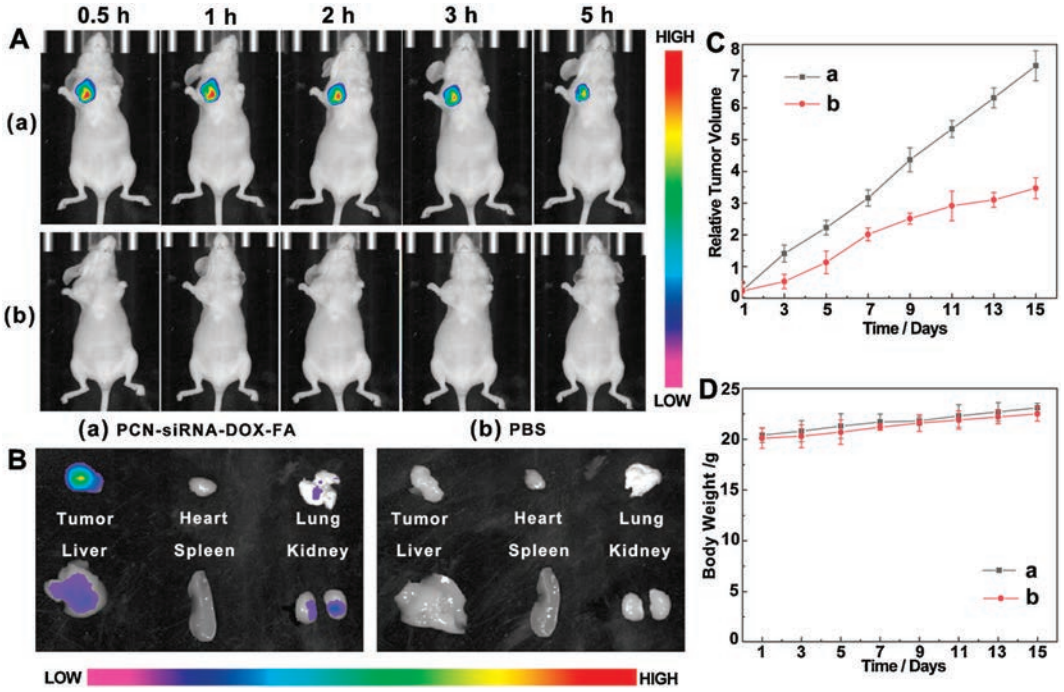

Fig. 4. (A) *In vivo* fluorescence images of tumor-bearing mice after treated with PCN-siRNA-DOX-FA complex (a) and PBS solution (b) from 0.5 h to 5 h. (B) Fluorescence images of bio-distribution in tumor, heart, lung, liver, spleen and kidney after treatment with of PCN-siRNA-DOX-FA complex (a) and PBS solution (b). (C) Relative volume change of tumor after different treatments from 1 day to 15 days: (a) treated with PBS solution, (b) treated with PCN-siRNA-DOX-FA complex. (D) The change curves of body weights during the treatments from 1 day to 15 days: (a) treated with PBS solution, (b) treated with PCN-siRNA-DOX-FA complex. Error bars indicate SD ($n = 3$).

complex based multi-channel treatment also achieved better performance on multi-therapy, which suggested the cooperative therapy will be one of the key points in nanomedicine. Although the application of low-toxicity nanomaterials in tumor diagnosis and treatment had obvious advantages, their metabolic pathways and organ accumulation problems still requires further research, the construction of degradable structures with bio-responsiveness in traditional carbon or silicon materials may be one of the effective solutions. On the other hand, achieving the selective analysis of intracellular bio-thiols and their real-time *in situ* monitoring was still a challenge in cancer early diagnosis.

Declaration of competing interest

The authors declare that they have no known competing financial interests or personal relationships that could have appeared to influence the work reported in this paper.

Acknowledgment

We acknowledge the support from the Project Fund for Shandong Key R&D Program (No. 2017GGX20121). The animal experiments have been approved by the Ethics Committee of the Key Laboratory of Optic-electric Sensing and Analytical Chemistry for Life Science, Ministry of Education.

Appendix A. Supplementary data

Supplementary material related to this article can be found, in the online version, at doi:https://doi.org/10.1016/j.cclet.2020.11.058.

References

[1] F. Bray, J. Ferlay, I. Soerjomataram, et al., CA Cancer J. Clin. 68 (2018) 394–424.
[2] W. Chen, R. Zheng, P.D. Baade, et al., CA Cancer J. Clin. 66 (2016) 115–132.
[3] C. Allemani, T. Matsuda, V. Di Carlo, et al., Lancet 391 (2018) 1023–1075.
[4] W. Fan, N. Lu, P. Huang, Y. Liu, et al., Angew. Chem. Int. Ed. 56 (2017) 1229–1233.
[5] Z. Hu, C. Fang, B. Li, Z. Zhang, et al., Nat. Biomed. Eng. 4 (2020) 259–271.
[6] L. Wang, Y. Chang, Y. Feng, et al., Nano Lett. 19 (2019) 6800–6811.
[7] Z. Chai, D. Ran, L. Lu, et al., ACS Nano 13 (2019) 5591–5601.
[8] J.F. Liao, Y.P. Jia, Y.Z. Wu, Wires Nanomed. NanoBiotech. 12 (2019) e1581.
[9] H. Chen, Z. Gu, H. An, et al., Sci. China Chem. 61 (2018) 1503–1552.
[10] L. Dykman, N. Khlebtsov, Chem. Soc. Rev. 41 (2012) 2256–2282.
[11] W. Yu, M. Shevtsov, X. Chen, H. Gao, Chin. Chem. Lett. 31 (2020) 1366–1374.
[12] Z. Shi, Q. Li, L. Mei, Chin. Chem. Lett. 31 (2020) 1345–1356.
[13] S. Zhang, X. Pei, H. Gao, et al., Chin. Chem. Lett. 31 (2020) 1060–1070.
[14] E. Blanco, H. Shen, M. Ferrari, Nat. Biotechnol. 33 (2015) 941–951.
[15] K.C.L. Black, Y. Wang, H.P, et al., ACS Nano 8 (2014) 4385–4394.
[16] Z. Yan, M. Cai, P.K. Shen, J. Mater. Chem. 22 (2012) 2133–2139.
[17] T. Wang, P. Zhang, Y. Sun, et al., Chem. Mater. 29 (2017) 4044–4051.
[18] M. Pirsaheb, S. Mohammadi, A. Salimi, et al., Microchim. Acta 186 (2019) 231–235.
[19] P. Zhang, Z.A. Qiao, S. Dai, Chem. Commun. 51 (2015) 9246–9256.
[20] D.S. Bin, Z.X. Chi, Y. Li, et al., J. Am. Chem. Soc. 139 (2017) 13492–13498.
[21] X. Ji, Z. Wang, S. Niu, C. Ding, Chem. Commun. 56 (2020) 5271–5274.
[22] D. Jaque, L. Martínez Maestro, B. Del Rosal, et al., Nanoscale 6 (2014) 9494–9530.
[23] H. Ehtesabi, Z. Hallaji, et al., Microchim. Acta 187 (2020) 150–156.
[24] Q. Zhu, M. Saeed, R. Song, et al., Chin. Chem. Lett. 31 (2020) 1051–1059.
[25] C. Ding, Y. Xu, Y. Zhao, et al., ACS Appl. Mater. Interfaces 10 (2018) 8947–8954.
[26] X. Wang, J. Sheng, M. Yang, Chin. Chem. Lett. 30 (2019) 533–540.
[27] R. van der Meel, E. Sulheim, Y. Shi, et al., Nat. Nanotechnol. 14 (2019) 1007–1017.
[28] L.P. Zhong, H. Zou, Y. Huang, et al., J. Biomed. Nanotechnol. 15 (2019) 352–362.
[29] J. Wu, D.H. Bremner, S.W. Niu, et al., J. Biomed. Nanotechnol. 15 (2019) 1415–1431.
[30] W. Xie, W.W. Deng, M. Zan, et al., ACS Nano 13 (2019) 2849–2857.
[31] S.H. Myers, V.G. Brunton, A. Unciti-Broceta, J. Med. Chem. 59 (2016) 3593–3608.